INFLIGHT SIMULATION OF SUSTAINED HIGH ROLL RATES USING A LOW ALPHA SPIN MODE: POTENTIAL APPLICATION TO AVIATION MEDICINE RESEARCH

A. P. Brown*, J Dillon*
***National Research Council, Canada**

Abstract

The Harvard Mk 4 research aeroplane of the NRC has been used to investigate spinning at a reduced angle-of-attack associated with normal spin recovery transition. The spin mode has potential as an inflight simulation tool for research into the physiological effects of sustained high roll rates. By the suitable manipulation of flight controls on the Harvard, the spin mode has been sustained for periods of 10-15 seconds, at spin rates of 220-270 °s^{-1}. The roll rate component is dominant in the low-α spin mode with roll rates p of ≥200 °s^{-1}, as high as 250 °s^{-1}, amounting to about eight roll revolutions. The aerodynamic forcing of the high roll-rate was attributed to attached flow on the left wing and separated flow on the right wing, as implied by inertial data analysis indicating that the out-of-turn wing angle of attack, α, was below stalling α, and confirmed by surface flow visualisation. Importantly for vestibular-occular research, the spin mode can be stopped sharply upon recovery. Translation of the acceleration vectors to the front and rear-seat pilot reference head positions indicated that the resultant gravitoinertial forces (GIF(R)) were essentially 1.1-1.2g, albeit *with ±8% anharmonic variation, canted rearwards 12° and 25° from the upright body position, respectively (*i.e. *equivalent to head-up canting at these angles). The roll-rate of the spin mode could be expected to excite vestibular-visual interactions, including the vestibulo-occular reflex (VOR), whilst viewing the wide FOV of the external scene, and post-rotary nystagmus, with only minor stimulation of the otolith. Other observed Harvard spin modes include the normal and higher-α modes, with p=90 °s^{-1} and 120 °s^{-1}, respectively, and with higher yaw rates. GIF(R) angles for the normal mode, equivalent to head-up tilt, were 11° and 37° for front and rear pilot head reference positions. The normal mode had ±13-15% harmonic variation in GIF(R) direction. The GIF(R) cant angles for the higher-α spin mode are substantially greater, equivalent to head-up tilts of 21° and 53°. Together, the low-α, normal and higher-α spin modes could provide a range of VOR excitation and post-rotary nystagmus, together with other reflexive interaction stimuli, for a range of vestibular axes stimulation, all with low levels of otolith stimulation. Finally, horizontally rolling (providing ±1g harmonic stimulation of the otolith) of the Harvard could be accomplished at a roll-rate of 90 °s^{-1}, for a sustained period of 8-10 seconds.*

1 Introduction

Traditionally, light aircraft spin modes have been classified as 'steep' or 'flat', the difference reflecting pitch attitudes associated with incidence (angle-of-attack, α) regimes: a steep spin mode is associated with moderate α, typically 40-50°, or 2-3 times the stalling α; in flat spin modes, α may be as high as 70-80°. For reasons of recovery ease, 'steep' modes are generally more desirable.

Often, during spin recovery, a temporary increase in spin rate precedes the abrupt discontinuation of spin rotation [1][2][3], as illustrated in Figure 1. Furthermore, the increase in spin rate is principally associated with an increase in roll rate.

If it were possible to sustain the high spin rate transient state associated with spin recovery, then relatively long-period applications of high roll rates could be achieved and possibly used for studies of physiological reflexes and interactions, such as vestibulo-occular, otolith-occular and cardiovascular-visual, during and post high roll-rate and subsequent hypergravity transition. This topic is a matter of on-going aviation medical research, particularly in relation to spatial disorientation events. Tactical military aircraft possess typical roll-rates within the range of 150 to 300°s^{-1}. However, given the types of research aeroplanes available, sustained roll rates at such magnitudes are difficult to achieve, typically due to cross-axis coupling (either pitch-roll or yaw-roll).

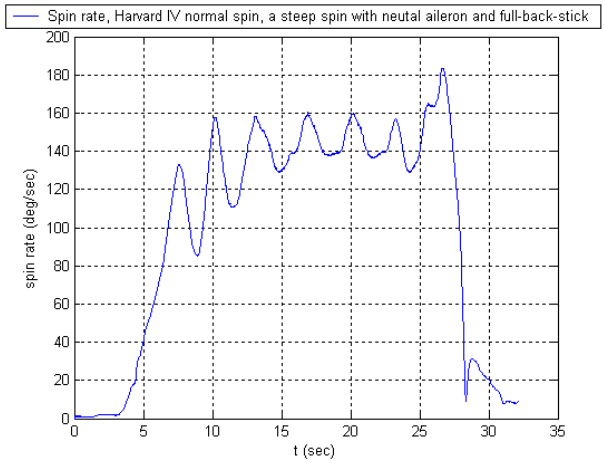

Figure 1 – spin rate of the NRC Harvard Mk IV basic trainer aeroplane, normal upright spin mode, *enroute* configuration.

The present flight research study was aimed at an examination of 'low-α' spin mode characteristics of the NRC Harvard Mk 4 flight research aeroplane.

2 Experimental Details

2.1 Research Aeroplane

The Harvard Mk 4 is a low-wing, single-engine, 1940's-era trainer, powered by the Pratt & Whitney R-1340 radial piston engine of 600 BHP. The NRC Harvard (shown inflight in Figure 2) continues to be used for continuation training and flight research projects. In external configuration, the aeroplane is essentially the same as that of the original Harvard Mk 4, with Mk 2 wings fitted, although the upper rear fuselage has been modified for the installation of various modern avionics antennae, including a GPS antenna mount. Internally, the NRC Harvard is equipped with a networked system of computers, including an Inertial Measurement Unit (IMU) system, located at the 5% MAC position, a data acquisition system (DAS) computer and a symbology generator (SG) computer, both located in the rear baggage bay.

Figure 2 – NRC Harvard aeroplane in winter flight over Ottawa. *(photo: H Turner, NRC)*

The SG computer drives the flat panel display in the rear cockpit, a head-down primary flight display (PFD) with engine power, air data and attitude-direction-indicator (ADI) inertial data information. This 'glass' rear cockpit has been used for unusual attitude (UA) recovery flight research [4].

The aerobatic weight limit is 5,490 pounds, at or below which, the Harvard may be used for non-inverted spinning flight (*i.e.* positive-α spins only). The characteristics of the normal spin (full-back-stick and full rudder, with neutral aileron) are 'steep' spin-typical. The spin entry phase is quite oscillatory, lasting about three turns. Residual oscillations may prevail, associated with some oscillatory buffet, more noticeable in the rear cockpit. Spin recovery, from the onset of standard recovery control application, takes 1½ to 2 turns. Compared to the right, left spins are significantly more oscillatory.

2.2 Instrumentation

Critical to the success of the flight research programme, the inertial reference system (IRS) was developed at NRC. It followed the architecture of earlier-developed NRC systems [5]. Principal IRS components consisted of a Honeywell HG1700 IMU, a NovAtel PwrPak-II-RT20 GPS receiver and an NRC-developed data recorder/processor (DRP).

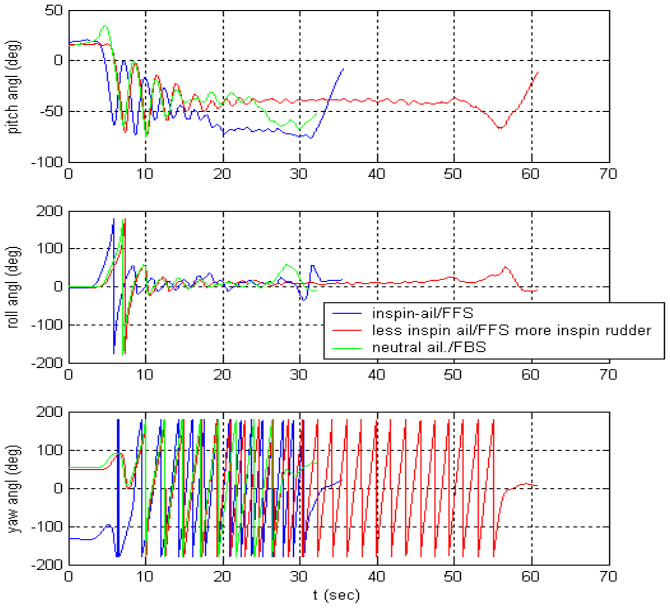

(a) Euler angles

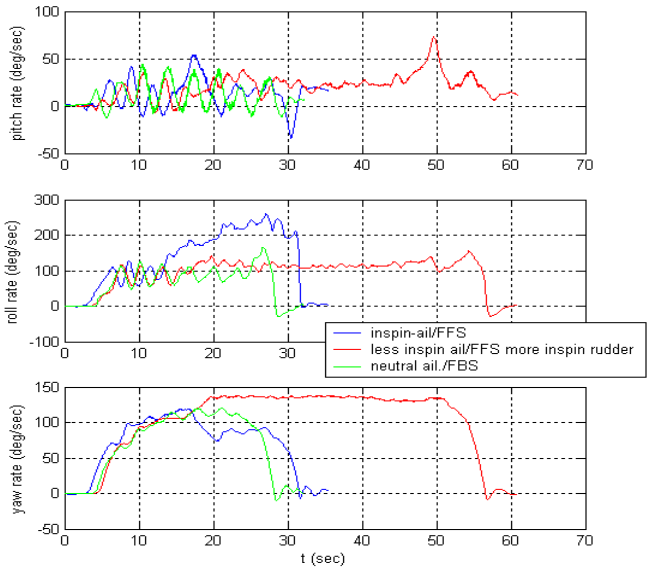

(b) angular rates

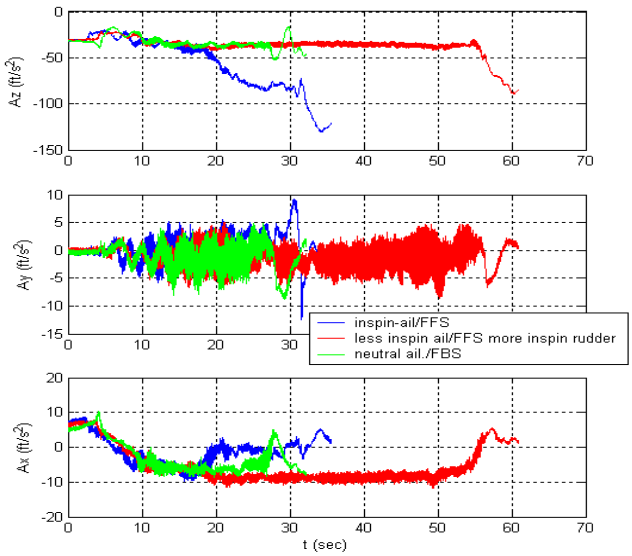

(c) IMU linear accelerations

Figure 3 – characteristics of three spin modes, for (i) inspin aileron/inspin rudder/FFS, (ii) less in-spin aileron/more in-spin rudder/FFS, and (iii) neutral aileron/full in-spin rudder/FBS (normal upright spin).

The DRP consisted of a TP400 single board computer from DSPDesign with a custom PC/104 interface board, together with a CompactFlash card for data recording. The system was powered from aircraft 28 Vdc using two DC/DC converters to provide 5 Vdc and ±15 Vdc.

The IMU outputs of incremental velocity and angle components were fed to the DRP, which used NRC-developed strapdown navigation software, coupled with an INS/GPS error state feedback Kalman filter, for the determination of a full set of outputs (*i.e.* Euler angles, angular rates, position, linear velocity and acceleration) at data rates as high as 600 Hz. Inertial responses to unsteady aerodynamic forces within a frequency range of 0 to 16Hz were of interest. Such responses were captured using an IMU data sampling rate of 64 Hz. GPS information was provided to the navigation computer from the rear-fuselage NovAtel GPS receiver. The GPS data, logged at 1 Hz, was used to calculate error state estimates, which were then fedback to correct the strapdown navigation calculations 'on the fly', after each Kalman filter measurement update.

Air data and control inceptor/surface positional information were not available for most of the flight programme, due to programme constraints. Angle-of-attack was derived from pitch angle (θ), velocity (V) and the vertical velocity (V_Z) component (assuming zero vertical wind component), $\alpha=\theta-V_Z/V$. For each wingtip, the helical angle-of-attack (α_{WT}) was derived from roll and yaw rates (p and r), $\alpha_{WT}=\alpha\pm Pb/2/\sqrt{\{V^2\pm((Rb/2)Cos\alpha)^2\}}$. Flights were generally conducted above inversion layers located at 5,000-7,000 feet in anti-cyclonic conditions, so that vertical wind components were likely to be less than ten knots. A vertical wind component of ±10 knots would equate to an error of about ±10% of stabilised spin α.

2.3 Low-α Spin Flight Test Matrix

The spin-rate flight research programme consisted of a progressive build-up of flight control inputs, in the normally stabilised spin to the right:

(1) full-back-stick (FBS) (normal spin control) with full-rudder and various amounts of out-spin and in-spin aileron;
(2) transitioning to full-forward-stick (FFS), and applying various amounts of aileron with reduced rudder deflection.

In every case, the incipient spin was entered with simultaneous FBS, full in-spin rudder and neutral aileron. Transition to FFS was effected after three turns.

3 Results and Discussion

3.1 FBS Spins

Compared to neutral aileron (normal spin control position), the usage of aileron in the FBS spin to the right resulted in essentially similar spin characteristics to those shown in Figures 1 and 3, with some transposition between yaw and roll rates – in other words, the spin rate varied little, but inspin aileron resulted in slightly increased roll rate and reduced yaw rate (roughly 10-15% with full-aileron), whilst outspin aileron reduced roll rate and increased yaw rate (by a similar amount). For inspin aileron deflection greater than about half-maximum, hinge-moment reversal (resulting in control force overbalance) abruptly occurred. At almost full inspin aileron, the overbalance control force was about 15 lbf (6.8 kgf).

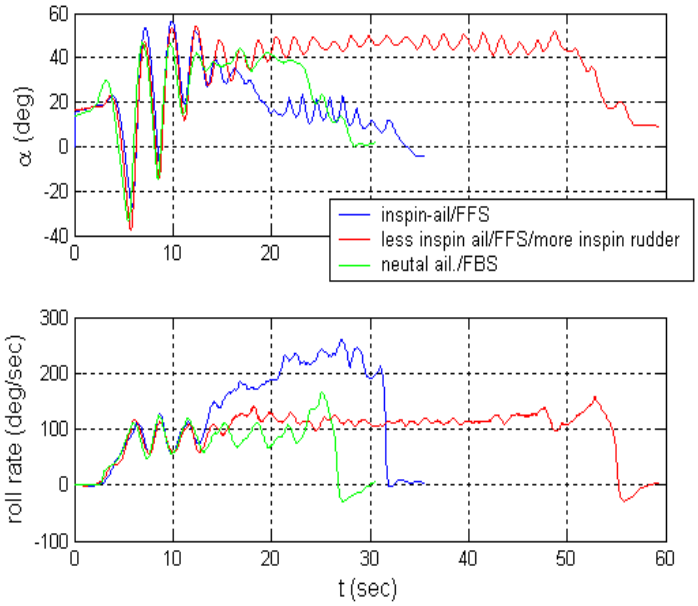

Figure 4 – derived α andmeasured roll-rate, three spins: neutral ail./FBS spin (*i.e.* normal spin) and two FFS spins, with slightly differing amounts of inspin aileron and outspin rudder.

3.2 FFS Spins

Abrupt or progressively-applied forward stick after only two spin rotations, tended to result in premature recovery from the spin. Progressively-applied forward stick after three rotations (applied at such a rate that FFS was achieved in about 1½ turns or 4-5 seconds duration) did not necessarily result in spin mode transition to the low-α mode. Co-ordinated reduction of inspin rudder deflection and application of inspin aileron was necessary, in order to achieve full transition to the low-α spin mode. Full transition was thus control technique sensitive, and occurred through an interim transition firstly to the higher-α spin mode. When full transition was achieved, modulation of elevator (some extent of back-stick from the FFS position) was necessary to maintain pitch attitude and prevent further nose-down change in pitch and spin discontinuation.

For example, Figure 4 shows derived-α and roll rate time-traces for three spins, with different flight control inceptor positions: normal spin (FBS/full-inspin rudder/neutral aileron) and two FFS/partial-inspin aileron and rudder combinations, both with FFS transition commencing after three rotations. For the two FFS spins, the roll-rate time-traces show the spin mode commencing to transition during the fourth rotation. However, after a half-turn the two traces diverge: the long-duration spin (red trace) stabilised with a roll-rate distinctly greater (about 25%) and a derived mean α about 15% higher than the normal spin (green trace); the other FFS spin (blue trace) progressively and fully transitioned to a low-α spin mode with a fuselage-centreline derived α of about 18°, and an undamped pitch oscillation component overlaid (concurrent with oscillatory buffet). The aeroplane conducted eight roll revolutions before recovery, in a time lapse of twelve seconds. During the transition to the low-α mode, the roll-rate progressively built-up, then remained anharmonically unsteady, with minima and maxima of about 215 and 265°/sec.

The correlation between the attractors of yaw rate and roll rate is shown in Figure 5 for the three spin modes, and tabulated below. By reference to the table, it is seen that unlike either of the other two spin modes, the low-α spin mode has a high roll:yaw ratio (2.77:1), such that the physiological response to the roll-rate, discontinuation thereof and 'g' application thereafter, would be less likely to be a cross-coupled (two-axis) or contaminated response.

Spin case	**Roll (P) rate**	**Yaw (R) rate**	**P:R ratio**
Neutral ail./FBS (**normal mode**)	85	115	0.74
Less inspin ail./FFS/more inspin rudder (**higher-α mode**)	115	133	0.86
Inspin ail./FFS (**low-α mode**)	230	83	2.77

With reference to pitch rate, Figure 3 displays the pertinent characteristics, the most significant difference being the regular harmonic oscillation of pitch rate in the normal spin mode, between –10 and 20°s^{-1}, compared to anharmonic variations of 20-40°s^{-1} in the higher-α spin and –10 to 20°s^{-1} in the low-α spin. In the low-α spin, θ was 65-75° nose-down. As shown in Fig.3, the normal acceleration loading at the IMU was greater, about 2.5g, primarily a consequence of the greater spin rate and greater nose-down attitude.

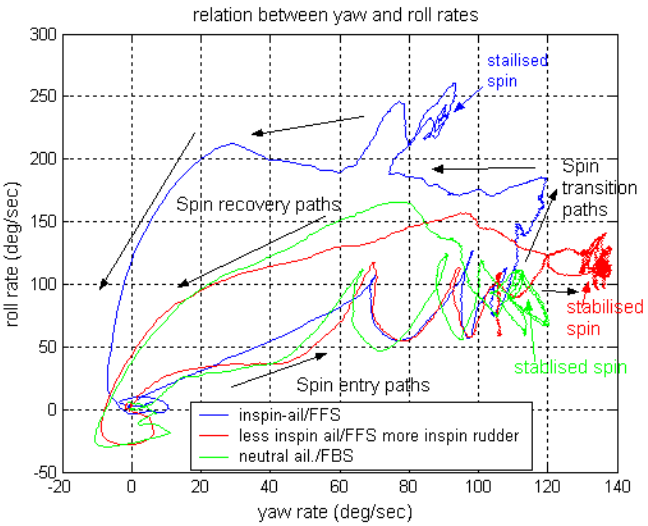

Figure 5 – relationship between roll and yaw rates in stabilised spins, for three spin modes, including the low-α mode.

3.3 Wingtip Helical α Analysis

The NRC Harvard low-α spin mode has the potential of being useful for physiological flight research. An explanation for the high roll-rate low-α spin characteristic can be found by considering α_{WT}, the derived behaviour of which is presented in Figure 6, for the three spin mode cases. Nominally, the wingtip helical angles of attack differ from the fuselage angle-of-attack by about ±20°. Of greatest significance, the transition path to the low-α spin mode appears (Fig.6(a)) to be associated with a reduction in the magnitude of the left wingtip helical angle of attack, to the stalling α magnitude of about 18°. Thereafter, the wingtip helical α is seen to reduce reasonably steadily to a value of about -4° (which could be expected to be about the sectional zero-lift α value), at which point the fuselage reference α is about the same magnitude as the stalling α. This observation tends to suggest that the left wing could be expected to have nearly fully attached flow.

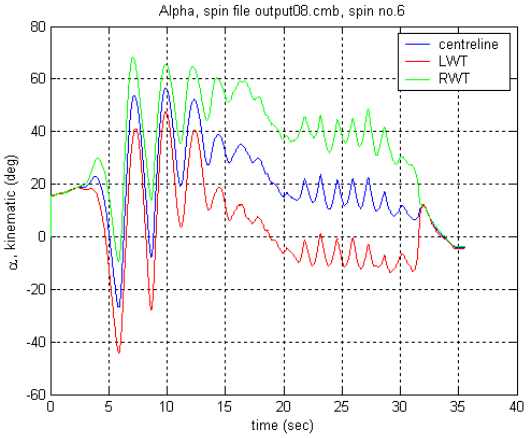

(a) Inspin-ail./FFS, low-α spin

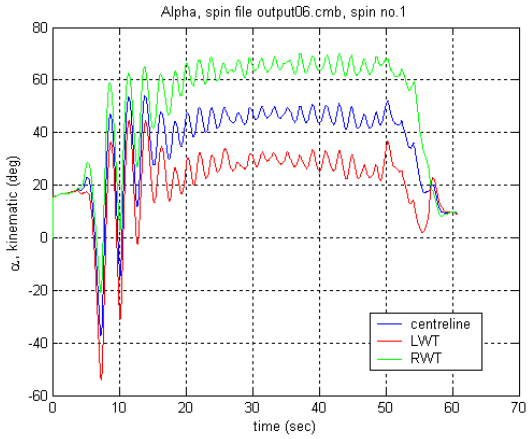

(b) less inspin ail./more rudder/FFS, higher-α spin

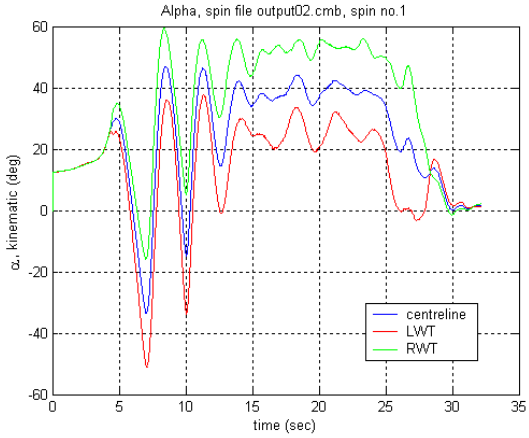

(c) normal spin mode (FBS/full inspin rudder/full inspin aileron)

Figure 6 – aeroplane centreline and in-spin/out-spin wingtip helical angles of attack.

Furthermore, it suggests that the oscillatory buffet experienced during the spin modes may be attributable to oscillatory right wingroot flow re-attachment and re-separation (the wingflow separation characteristics of the aeroplane during straight flight stall were a wingtip onset and a migration to wingroot).

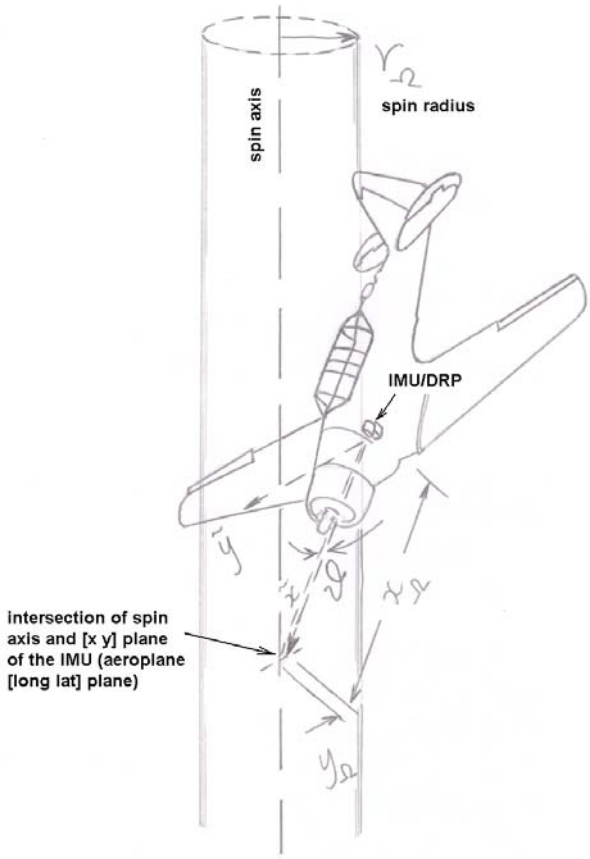

Figure 7 – spin axis geometry, in relation to the fuselage centreline (x axis); low-α mode shown, with off-CG (forward-displaced) spin axis position and [x_Ω y_Ω] roughly to scale. [for this spin axis position, diag. basis from Refs. 6,7 and 8].

3.4 Spin Axis Position

The spin axis position, in the lateral plane of the aeroplane (parallel to the [x y] orientation of the IMU), can be described by the distance increment vector $\tilde{n}=[x_\Omega\ y_\Omega]$ from the IMU station, FS72. The spin radius (from the IMU) will then be related to $\tilde{n}$ by the spin pitch angle, as diagrammatically depicted in Figure 7.

The spin axis positional vector $\tilde{n}$ with respect to the IMU position can be estimated from the IMU-measured linear acceleration data or from IMU-derived position [5] whilst spinning (spin tracks). For an inter-comparison, both methods shall be briefly presented.

Linear acceleration analysis shall be considered firstly. For steady angular rates (*i.e.* excluding the spin entry and recovery phases), the accelerations can be related to the principal kinematic components as:

$$\begin{aligned} a_X &= gCos\phi Sin\theta + (\Omega^2 r_\Omega)[Cos\theta Cos\vartheta + Cos\phi Sin\theta Sin\vartheta] \\ a_Y &= gSin\phi + (\Omega^2 r_\Omega)[Cos\theta Sin\vartheta] \\ a_Z &= gCos\phi Cos\theta + (\Omega^2 r_\Omega)[Sin\theta Cos\vartheta + Sin\phi Sin\theta Sin\vartheta] \end{aligned} \quad (1)$$

For the solution of ϑ and r_Ω (and hence $\tilde{n}$) the system of equations is redundant. The a_X and a_Y equations have been manipulated to solve for ϑ and r_Ω. [ϑ r_Ω] is related to $\tilde{n}$ by noting Tan $\vartheta = y_\Omega/x_\Omega$ and r_Ω = {Cos ϕ Cos θ / Cos ϑ} x_Ω. The solutions for [ϑ r_Ω] for the three spin modes of Figures 3 and 4 resulted in the following mean values:

Spin case	**ϑ (deg)**	**r_Ω m (ft)**
Normal, neutral ail./FBS (**normal mode**)	25	0.7 (2.3)
Less inspin ail./FFS/more inspin rudder (**higher-α mode**).	40	0.43 (1.4)
Inspin ail./FFS (**low-α mode**)	0	1.22 (4)

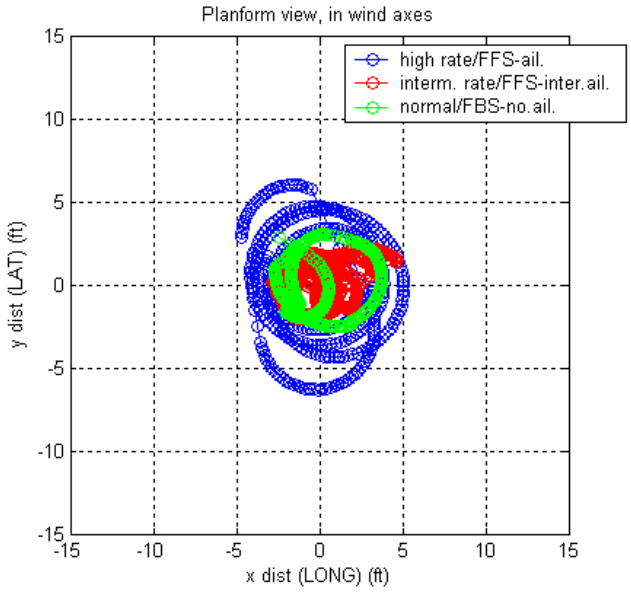

Figure 8 – estimated ground spin tracks with wind drift extracted by linear regression of [long lat] drift during spins, for the low-α normal and higher-α spin modes.

The spin radius values were successfully compared to those determined from the aeroplane geographic position, with wind-drifts extracted by linear regression over the stabilised spin portions of the flight tracks, leaving an estimate of the spin tracks in zero-wind conditions. The resultant tracks of the IMU are presented in Figure 8. It is seen that the low-α track (blue) had some extent of horizontal wander, but was reasonably circular, with r_Ω=[0.73 0.52 1.43]m. An elliptical track could be expected to exacerbate harmonic variations in rates and accelerations.

3.5 Pilot Head GIF Environments, Per-spin

For flight research into vestibular-occular, otolith-occular and cardiovascular-occular interactions, the linear accelerations applied to the handling pilot are of required interest. With reference to the IMU position, the low-α spin mode had a larger spin radius and a larger nose-down pitch angle. The latter tended to offset the spin radius, in relation to the resultant gravitoinertial acceleration vector (GIF(R)) applied to the pilots.

Figure 9 – sideview of the Harvard in flight, highlighting the front and rear pilot head reference positions.
[photo: John R Davies, Ottawa]

As shown in Figure 9, the front and rear seat pilots are seated quite high above the fuselage centerline – pilot head reference positions are about 0.84 m (2.76 feet) above the IMU position. Accordingly, when the linear acceleration vectors were translated to the front and rear pilot head reference positions, the magnitudes and pitch orientations, with respect to the pilot-upright position, of the resultant GIF(R) vectors are shown in Figure 10 for the front and rear pilot head reference positions.

For the low-α spin mode, the magnitude of the GIF(R) vector at both pilot-head reference positions was close to 1g, with slight anharmonic temporal variations ($\pm$8%). In the

fore-aft direction, the GIF(R) vector was orientated somewhat aft of the pilot-upright position, the magnitude of $\theta_{GIF(R)}$ being greater for the rear pilot head position and for greater yaw rates. The normal spin mode had harmonic variation of $\pm$13-15% magnitude in GIF(R) orientation. For the three spin modes **[low-α normal higher-α]** , $\theta_{GIF(R)}$ = [-12° -11° -21°] [-25° -37° -53°] at the P1 and P2 reference head position, respectively.

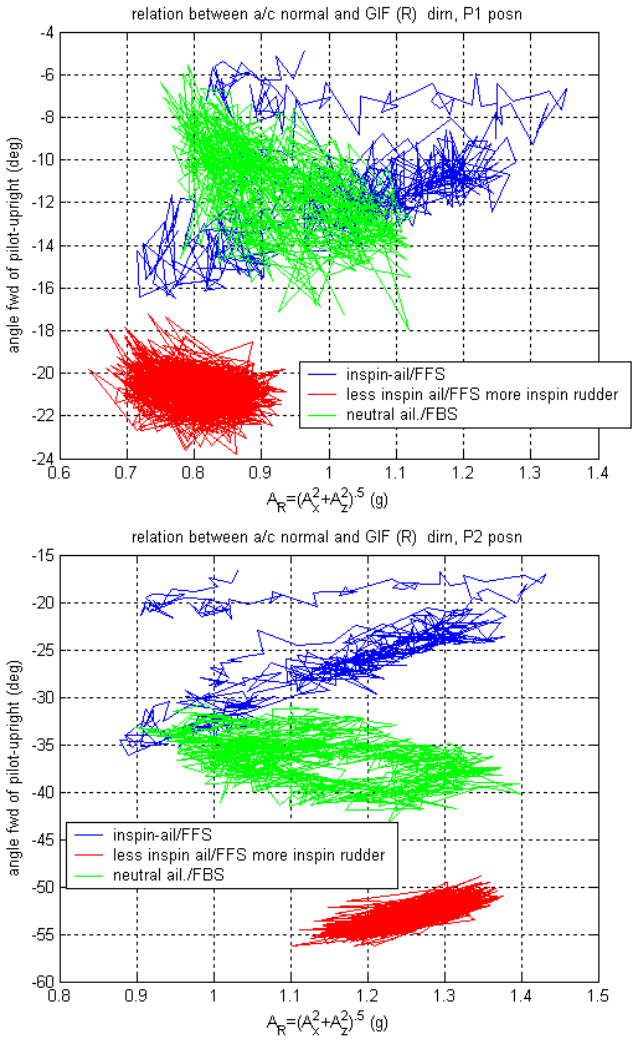

Figure 10 – GIF(R) magnitude, A_R and fore-aft orientation, with respect to pilot upright ('neg' sign is aft of the upright) for front (P1) and rear (P2) pilot head reference positions, during the three spin modes.

The sideways angular orientation of the GIF(R) vector with respect to the pilot upright position, $\Psi_{GIF(R)}$, was low for all spin modes: 5° with no effective variation for the low-α spin mode, 2.5°$\pm$7.5° for the normal mode and 5°$\pm$7.5° for the higher-α spin mode.

In relation to the low-α spin mode in particular, the quantification of Figure 10 and the low sideways orientation of the GIF(R) agree with the qualitative observations of spin sensations by the first author as project test pilot; in particular, the P1 position 'rolling at the centre of rotation' sensation was strong and diminished the sensation of yaw, whilst the 'g' sensation was similar to that whilst being normally seated upright, with no apparent feel of harmonic 'g' variation.

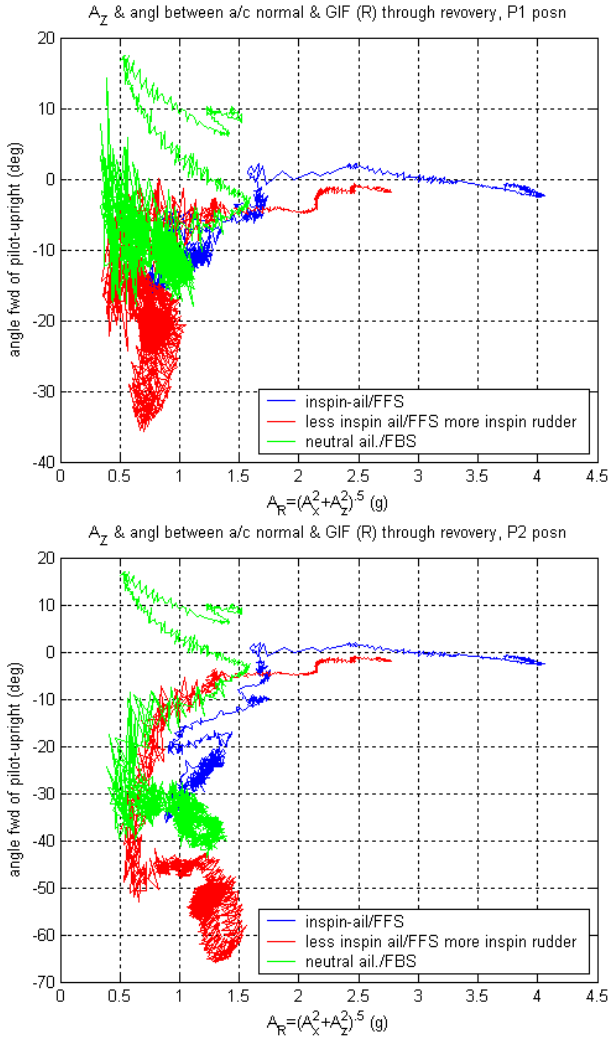

Figure 11 – GIF(R) magnitude and fore-aft orientation with respect to pilot-upright for front (P1) and rear (P2) pilot head positions, per and post-spin for each of the three spin modes.

3.6 Pilot Head GIF Environments, Post-spin

Figure 11 (compared to Figure 10) presents expanded maps of GIF(R) magnitude and orientation with respect to pilot-upright, which

cover the post-spin pitch-up. Differing post-spin hypogravity to hypergravity transition pitch-up manoeuvres have been executed for the spin examples shown, but they are not spin mode dependent.

Comparing the spin recovery segments themselves: the low-α spin recovery is essentially a >1g recovery (with an 'immediate' spin cessation, taking <1 second, compared to ≈5 sec. for the normal mode and ≈7 seconds for the higher-α mode), whereas the normal and higher-α mode recoveries track to 0.5g during the recovery phases. Post-spin, a 4g pitch-up was conducted for the low-α spin example; 2.8g for the higher-α spin example and, for the normal spin mode example, 1.6g at spin-stop, a pitch-down to 0.5g followed by a 1.5g pitch-up.

Considering the very prompt recovery from the low-α spin mode, the first author's observations as project test pilot are significant. They indicate that a self-awareness of torsional (post-roll) nystagmus was not predominant, rather the sensation of post-rotary angular rate saturation of the nasooccipital vestibular axis was overwhelming. Momentary vision impairment in the form of loss of definition and of colour resolution occurred occasionally, concurrently with the rate sensation.

3.7 Application to Aviation Medical Research

The functioning and reflexive responses of the vestibular, visual, somatosensory and cardiovascular systems, and interactions there-between during manoeuvring, which involves linear acceleration changes, angular rates and angular accelerations, have been a matter of research for some time and are a matter of on-going concern, for example in relation to spatial disorientation (SD) during both low-rate piloting and the high-rate tactical manoeuvring pilot environment of military aeroplanes in visual meteorological conditions (VMC) [9][10][11]. Cheung [12] provides a summary of sensory reflexive and interactive responses being potentially contributory to SD. Benson and Guedry [13] noted the interference to vision produced by nystagmus stimulated by separate sinusoidal pitch and yaw rate (covering a peak rate range of $\pm$60 to $\pm$159°s^{-1}). Melvill Jones *et al* [14] measured the differing yaw, pitch and roll vestibular responses and considered their flight implications. Inflight research [15] has provided a consistent demonstration of post-roll vestibular illusionary effects, whilst the potential SD problem of overall physiological responses per and post sequential or concurrent rolling and pitch ('G') manoeuvring, and the research need pertaining thereto, are elucidated by Cheung *et al* [9].

The spin and manoeuvre characteristics of the NRC Harvard, together with the research flight instrumentation, data acquisition and rear-cockpit display systems, offer the possibility of a number of experimental scenarios, for full-flight research of vestibulo-ocular, otolith-ocular and cardiovascular-ocular interactions, in high manoeuvre environments:

Low-α spin mode: during and post sustained high roll-rate (>200°s^{-1}), with comparatively low yaw rate, low effective head tilt from upright, only minor otolith excitation, and various post-rotary pitching 'g' levels between 1.8g and 5g: for

- no attitude display information (rear pilot seat),
- a synthetic wide FOV of a primary flight display attitude indicator on the rear cockpit flat panel display, artificially indicating zero pitch but driven at the aeroplane roll-rate (rear pilot seat), and
- full external visual reference (front and rear pilot seat positions).

Normal and higher-α spin modes: intermediate roll rate and yaw rate combinations in the range of 90°s^{-1} to 150°s^{-1}, again with only minor otolith stimulation, but with greater effective head-up tilt angles.

Aileron roll manoeuvres: providing roll rates of 90°s^{-1} for 10 seconds with harmonic ($\pm$1g) otolith stimulation; and

Barrel roll manoeuvres: providing low combined roll and yaw rates (both about 30°s^{-1}), with only minor otolith stimulation, and no effective head-up or down tilt.

4 Conclusions

A flight research investigation of a low-α spin mode of the NRC Harvard has been conducted. The low-α mode of spinning has been stabilised and sustained for 10-15 seconds, at a spin rate of 220-270 deg/sec. The spin mode was largely roll-rate, within the range of 200-250 deg/sec, with peak values as high as 265 deg/sec. Note that 10-15 seconds of sustained operation equates to about eight roll revolutions. The duration and number of revolutions is greater than that generally possible on tactical military aircraft; therefore, the mode provides an inflight simulation platform for full-flight research into the reflexive and interactive effects amongst the vestibular, visual and somatosensory systems of sustained high roll-rate, abrupt discontinuation of high roll rates, and g-application following roll-rate discontinuation.

Acknowledgements

In relation to the success of the integrated INS/GPS navigation system, the foundation and formative work of Barrie Leach, NRC, is greatly acknowledged. Acknowledgement is also given to NRC colleague Rob Erdos, who provided the 'pivotal' demonstration of the NRC Harvard's FFS/outspin aileron spin mode characteristics, and also to NRC colleagues Dr Greg Craig and Sion Jennings. The investigative project was initiated under the Memorandum of Understanding between the NRC and the DRDC of the Department of National Defence of Canada, monitoring provided by Dr Bob Cheung, Toronto DRDC.

References

[1] Stough, H.P., III, "Flight Investigation of Stall, Spin and Recovery Characteristics of a Low-Wing, Single-Engine, T-Tail Light Aeroplane," *NASA Technical Paper 2427*, May 1985.

[2] Brown, A.P., "Certification Flight Test Report on the Inadvertent Spin Handling of the Eagle X-TS Aeroplane when considered against the Requirements of JAR-VLA 221," *Australian Flight Test Services Pty Ltd report 921/13 (10), 27 April 1993.*

[3] Stough, H.P., Patton, J.M., Jr, "The Effects of Configuration Changes on Spin and Recovery Characteristics of a Low-Wing General Aviation Research Airplane," *AIAA Aircraft Systems and technology Meeting, New York, New York, 20-22 August 1979*, Paper No. AIAA-79-1786.

[4] Craig, G., Erdos, R. and Cheung, B., "Development of an Airborne Display Research Facility," *SAE 03WAC-5, SAE World Aviation Congress, 2003, Montreal.*

[5] Leach, B.W., Rahbari, R. and Dillon, J., "Development of a Real-Time Strapdown Inertial / GPS Integrated Navigation System," *NRC-CNRC Report LTR-FR-194,* December 2002.

[6] Hill, S.D. and Martin, C.A., "A Flight Dynamic Model of Aircraft Spinning," *Aeronautical Research Laboratory, Defence Science and Technology Organisation, Department of Defence, 1990*, Flight Mechanics Report 180, AR-005-600.

[7] Martin, C.A., "The Spinning of Aircraft – A Discussion of Spin Prediction Techniques Including a Chronological Bibliography," *Aeronautical Research Laboratory, Defence Science and Technology Organisation, Department of Defence, 1988*, Aerodynamics Report 177, AR-005-530.

[8] Bowman, J.S., Jr., "Summary of Spin Technology as Related to Light General-Aviation Airplanes," *NASA Technical Note, 1971*, NASA TN D-6575.

[9] Cheung, B., Ercoline, B. and Metz, P., "G-Transition Induced Loss of orientation and Reduced G Threshold," *Spatial Disorientation in Military Vehicles: Causes, Consequences and Cures, 2003*, NATO Research and Technology Organisation, RTOMP-086.

[10] Knapp, C. J. and Johnson, R., "F-16 Class A Mishaps in the U.S. Air Force, 1975-93," *Aviation Space Environment Medicine, 1996.*

[11] Johnson, K.R., "Spatial Disorientation in Military Aviation," *Naval Aerospace medical Research Laboratory, Pensacola Florida presentation*, November 2000.

[12] Cheung, B., "Non-visual Spatial Orientation Mechanisms," Defence Research and Development Toronto, Canada presentation.

[13] Benson, A. J. and Guedry, F. E., "Comparison of Tracking-Task Performance and Nystagmus During Sinusoidal Oscillation in Pitch and Roll," *NASA Technical Aerospace Medicine*, V.42, No.6, June 1971.

[14] Melvill Jones, G., Barry, W. and Kowalsky, N., "Dynamics of the Semicircular Canals Compared in Yaw, Pitch and Roll," *Aerospace Med., 1964:984-989.*

[15] Ercoline, W. R., "Post-Roll Effects on Attitude Perception: 'The Gillingham Illusion'," *Aviat Space Environ Med 2000; 71: 489-95.*